Malaysian Journal of Analytical Sciences, Vol 21 No 4 (2017): 889 - 900
DOI: https://doi.org/10.17576/mjas-2017-2104-15

MALAYSIAN JOURNAL OF ANALYTICAL SCIENCES
Published by The Malaysian Analytical Sciences Society
ISSN 1394 - 2506

SYNTHESIS OF ZnO/rGO NANOHYBRID FOR IMPROVED PHOTOCATALYTIC ACTIVITY

(Sintesis Nanohibrid ZnO/rGO Untuk Mempertingkatkan Aktiviti Fotopemangkinan)

Marilyn Yuen Sok Wen[1], Abdul Halim Abdullah[1,2]*, Lim Hong Ngee[1]

[1]*Department of Chemistry, Faculty of Science*
[2]*Materials Science and Characterization Lab., Institute of Advanced Technology*
Universiti Putra Malaysia, 43400 UPM Serdang, Selangor, Malaysia

**Corresponding author: halim@upm.edu.my*

Received: 20 September 2016; Accepted: 16 May 2017

Abstract

Nanohybrids of zinc oxide/reduced graphene oxide (ZnO/rGO) with varying graphene oxide content were prepared via precipitation and were subsequently utilised in the photodegradation of methyl orange (MO) under UV light irradiation. The prepared photocatalysts were characterized by X-ray Diffraction (XRD), Field Emission Scanning Electron Microscopy (FESEM), Transmission Electron Microscopy (TEM) and Raman spectroscopy. The surface area and the band gap energy of the photocatalysts were determined by the Brunauer-Emmett-Teller method and UV-visible spectroscopic analysis. The ZnO/rGO nanohybrids produced had smaller particle sizes and lower band gap energy than that of ZnO. All the ZnO/rGO nanohybrids demonstrated better photocatalytic efficiency in the photodegradation of MO compared to ZnO. ZnO/rGO10 exhibited the highest photocatalytic activity with a rate constant that was four times higher than pure ZnO and about 40% enhancement in the photocatalytic activity for the removal of methyl orange within 3 hours. The enhanced photocatalytic performance of the ZnO/rGO photocatalysts was due to the efficient transfer of photogenerated electrons to the graphene sheet that inhibited the recombination of electron-hole pairs.

Keywords: zinc oxide, reduced graphene oxide, nanohybrid, precipitation method, photocatalysis

Abstrak

Nanohibrid zink oksida/grafin oksida terturun (ZnO/rGO) dengan kandungan grafin oksida yang berbeza telah disediakan melalui kaedah pemendakan dan seterusnya digunakan dalam fotodegradasi metil jingga (MO) di bawah sinaran cahaya UV. Fotopemangkin yang disediakan telah dicirikan dengan menggunakan pembelauan sinar-X (XRD), mikroskopi pengimbasan elektron (FESEM), mikroskopi transmisi elekron (TEM) dan spektroskopi Raman. Luas permukaan dan tenaga jurang jalur fotomangkin telah ditentukan menggunakan kaedah Brunauer-Emmett-Teller dan analisis spektroskopi UV-sinar nampak. Nanohibrid ZnO/rGO yang terhasil mempunyai saiz zarah yang lebih kecil dan tenaga jurang jalur yang lebih rendah berbanding dengan ZnO. Nanohibrid ZnO/rGO mempamerkan kecekapan fotopemangkinan yang lebih tinggi dalam fotodegradasi MO berbanding dengan ZnO. ZnO/rGO10 mencatatkan aktiviti fotopemangkinan yang tertinggi dengan pemalar kadar empat kali ganda lebih tinggi daripada ZnO dan peningkatan 40% dalam aktiviti fotopemangkinan degradasi metil jingga dalam masa 3 jam. Peningkatan prestasi fotopemangkinan pemangkin ZnO/rGO adalah disebabkan oleh kecekapan pemindahan fotojanaan elektron ke lembaran grafin yang seterusnya menghalang penggabungan semula pasangan elektron-lubang.

Kata kunci: zink oksida, grafin oksida terturun, nanohibrid, kaedah pemendakan, fotopemangkinan

Introduction

Water pollution due to effluents from textile industries, especially dyes is a cause of serious concern. It is estimated that 1% to 15% of the dye is lost during the dyeing processes which is subsequently released into natural water resources and the wastewater system [1]. When released into the water, dyes may change the colour of the water, impact light penetration and reduce the solubility of gases [2].This in turn, has a serious impact on the aquatic ecosystem. Dyes are also stable and difficult to be biodegraded due to their synthetic origins and complex aromatic structures [3]. Hence, it is important to treat water resources and wastewaters containing such organic pollutants. Photocatalysis has long been introduced as a means of water decontamination [4]. Photocatalysis involves utilizing electron- hole pairs generated upon the irradiation of light to degrade organic molecules adsorbed on the surface of the photocatalyst [5]. This green technique can be performed in an ambient environment and may also oxidize organic carbon into carbon dioxide [6].

The use of zinc oxide (ZnO) as a photocatalyst has several advantages including a low production cost, wide band gap (~3.37 eV), high stability and catalytic activity, better sensitivity in UV light and the presence of its many active sites with high surface reactivity [7-9]. However, the fast recombination of the electron-hole pairs of ZnO has limited its catalytic efficiency [10]. Recently, many attempts have been carried out to enhance the performance of ZnO photocatalysts by modifications with noble metal loading, ion doping or the incorporation of electron-accepting materials to extend the light absorption range to the visible light region or to suppress the electron–hole recombination process [11].

Graphene, a two-dimensional (2D) single-layered carbon sheet with an sp^2 network of carbon atoms has excellent conductivity, good chemical stability, mechanical flexibility, a high mobility of charge carriers and a large specific surface area [12].These properties enable graphene to be an ideal support in combination with semiconductor photocatalysts. Graphene can be prepared by reducing graphene oxide (GO) [13]. The presence of oxygen-containing functional groups on the surface of the reduced graphene oxide (rGO) also makes graphene an excellent supporting material by anchoring strongly to the metal oxide nanostructure [14, 15].

Many methods have been used to fabricate ZnO photocatalysts hybridised with rGO, including solvothermal [16], chemical deposition [11], hydrothermal [15, 17, 18] and sol- gel [19] methods. Herein, we report a simple precipitation method to prepare ZnO/rGO nanohybrids with zinc acetate dihydrate and graphene oxide (GO) as the starting materials, and ammonia as both the precipitator and reductant. This study is focused on determining the effect of rGO on the structure and photocatalytic activity of ZnO.

Materials and Methods

Materials

Zinc acetate dihydrate ($(CH_3COO)_2Zn.2H_2O$) and 25% ammonia solution (NH_3) were purchased from Merck. Methyl orange (MO) ($C_{14}H_{14}O_3N_3SNa$), a model pollutant, was obtained from Bendosen. All chemicals were used without further purification.

Synthesis of graphene oxide

GO was synthesized using a modified Hummers method [20]. In a typical experiment, graphite flakes, H_2SO_4:H_3PO_4 (320:80 ml) and $KMnO_4$ (18g) were mixed together under magnetic stirring. The mixture was stirred for 3 days to allow the oxidation of graphite, where the colour of the mixture changed from dark purplish green to dark brown. The colour of the mixture changed to bright yellow after the addition of H_2O_2 solution. The graphite oxide formed was washed three times with 1M HCl aqueous solution and repeatedly with deionized water using a centrifugation force of 10,000 g until wash-water with a pH of 4 – 5 was obtained.

Preparation of ZnO/rGO nanohybrid photocatalyst

The ZnO/rGO nanohybrid was synthesized by mixing 10 ml of 1mg/ml GO with 100 ml 0.3M zinc acetate dihydrate solution followed by the addition of ammonia solution until a pH 10 of was achieved. The precipitate was later filtered and washed several times with deionised water and dried overnight in an oven at 100 °C. The dried powder was then calcined at 400 °C for 2 hours and labelled as ZnO/rGO10. In order to study the effect of GO content on the physicochemical properties and photocatalytic activity, three different nanohybrids were prepared by

changing the initial volume of the GO solution. ZnO/rGO nanohybrids with a volume ratio of 5:100, 10:100 and 20:100 of GO and Zinc acetate dihydrate solution were denominated as ZnO/rGO5, ZnO/rGO10 and ZnO/rGO20. For comparison, pure zinc oxide (ZnO) was also obtained using the same method without adding any GO.

Characterization

The phase and crystallinity of the samples were analysed using Philips PW 3040/60 MPD X-ray diffractometer with Ni-filtered CuK_{α} radiation. The X-ray diffraction (XRD) pattern were recorded in the 2θ range of 20° - 80° at a scanning rate of 2°/min. The surface morphology of the samples was studied using Field Emission Electron Microscopy (FESEM) (FEI Nova Nanosem 230 combined with EDX) and Transmission Electron Microscopy (TEM) (Hitachi H-7100). The surface area of the samples was determined using a BET surface area analyzer (BELSorp Mini II). Raman spectroscopy (WITec Alpha 300R) was used to study the disordered crystal structure of the carbon based material and to confirm the presence of rGO. Diffuse reflectance spectra were recorded using a Shimadzu UV-3600 spectrophotometer in order to determine the band gap energy of the prepared samples.

Photocatalytic activity experiment

The photocatalytic performance of the prepared photocatalysts was evaluated in the photodegradation of methyl orange (MO) under the illumination of a 6W UVA lamp for 3 hours. In a typical experiment, 0.5g of photocatalyst was suspended in a photoreactor containing 500 ml of MO solution (10 ppm). The resultant solution was magnetically stirred in the dark for 30 minutes to reach an adsorption-desorption equilibrium prior to UV irradiation. An amount 5 ml of test samples were taken at predetermined time intervals and were immediately filtered with a 0.45 µm cellulose nitrate filter. The concentration of MO in the test samples was determined (Perkin Elmer Lambda 35 UV-Vis Spectrometer) at a wavelength of 464.3 nm.

Results and Discussion

X-ray diffraction

Figure 1 displays the XRD patterns of pure ZnO and ZnO/rGO nanohybrid photocatalysts. The diffraction peaks observed in the XRD pattern of the prepared photocatalysts were consistent with the hexagonal wurtzite phase of ZnO (JCPDS No. 36-1451). The peaks at 2θ=31.8°, 34.4°, 36.2°, 47.5°, 56.6°, 62.8°, 66.4°, 68.0°, 69.1°, 72.5° and 77.0° are associated with the 100, 002, 101, 102, 110, 103, 200, 112 and 203 crystalline planes of ZnO, respectively. However, no characteristic peak for rGO was observed in the XRD patterns due to its low content and its relatively low diffraction intensity compared to ZnO [21-23]. The average crystallite size of ZnO and the ZnO/rGO nanohybrid photocatalysts was calculated using Scherrer's equation and the data is shown in Table 1. It was also observed that the intensity of the diffraction peaks of the ZnO/rGO nanohybrids decreased as the rGO content increased. This indicated that the crystallinity of ZnO deteriorated as the concentration of ZnO in the ZnO/rGO nanohybrids decreased when compared to pure ZnO [24]. Kuo and co-workers [25] reported that an increase in the concentration of the dopant led to the formation of stresses because of the difference in ionic size of zinc and the dopant. ZnO/rGO nanohybrids were observed to have smaller crystallite sizes when compared to pure ZnO. This was due to the presence of the dopant, (rGO) which hindered the growth of crystal grains[26].

Table 1. Physical characteristics of ZnO and ZnO/rGO nanohybrids.

Photocatalyst	Crystallite Size (nm)	Surface Area (m^2g^{-1})	Band Gap Energy (eV)
ZnO	43	5.15	3.16
ZnO/rGO5	32	7.78	3.05
ZnO/rGO10	36	9.70	3.08
ZnO/rGO20	32	7.48	3.05

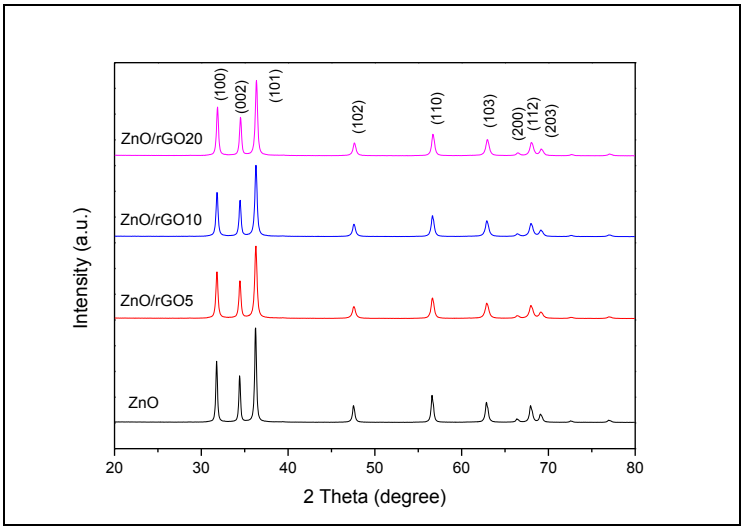

Figure 1. XRD patterns of ZnO and ZnO/rGO nanohybrid photocatalysts

Morphology

The surface morphology of the ZnO and ZnO/rGO nanohybrid photocatalysts, determined using TEM and FESEM, is shown in Figures 2 and 3, respectively. TEM images revealed the presence of ZnO on the surface of the graphene sheet. The ZnO nanoparticles were nearly spherical in shape, self-assembled and were randomly distributed on the graphene sheets. The formation of spherical ZnO nanoparticles could have been due to the addition of OH^- that increased the reaction rate, thus forming more nuclei in a short time [5]. The two- dimensional graphene sheets were not perfectly flat but rough with wrinkles. EDX were used to distinguish the components present in the samples. As shown in Figure 4, carbon (C), zinc (Zn) and oxygen (O) were the main elements present in the ZnO/rGO nanohybrid photocatalysts with no unexpected elements being detected. This confirmed the purity of the samples.

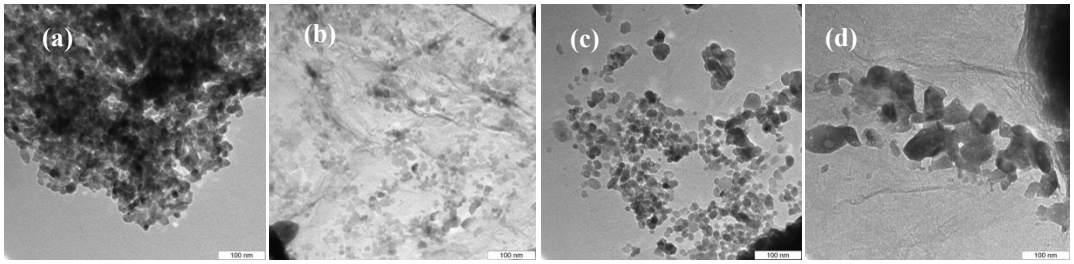

Figure 2. TEM images of (a) ZnO, (b) ZnO/rGO5, (c) ZnO/rGO10 and (d) ZnO/rGO20

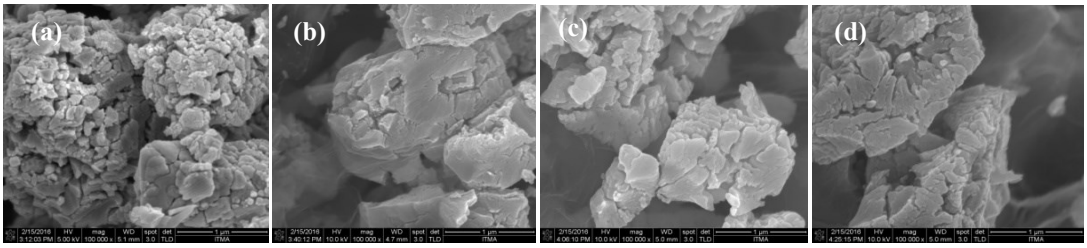

Figure 3. FESEM images of (a) ZnO, (b) ZnO/rGO5, (c) ZnO/rGO10 and (d) ZnO/rGO20

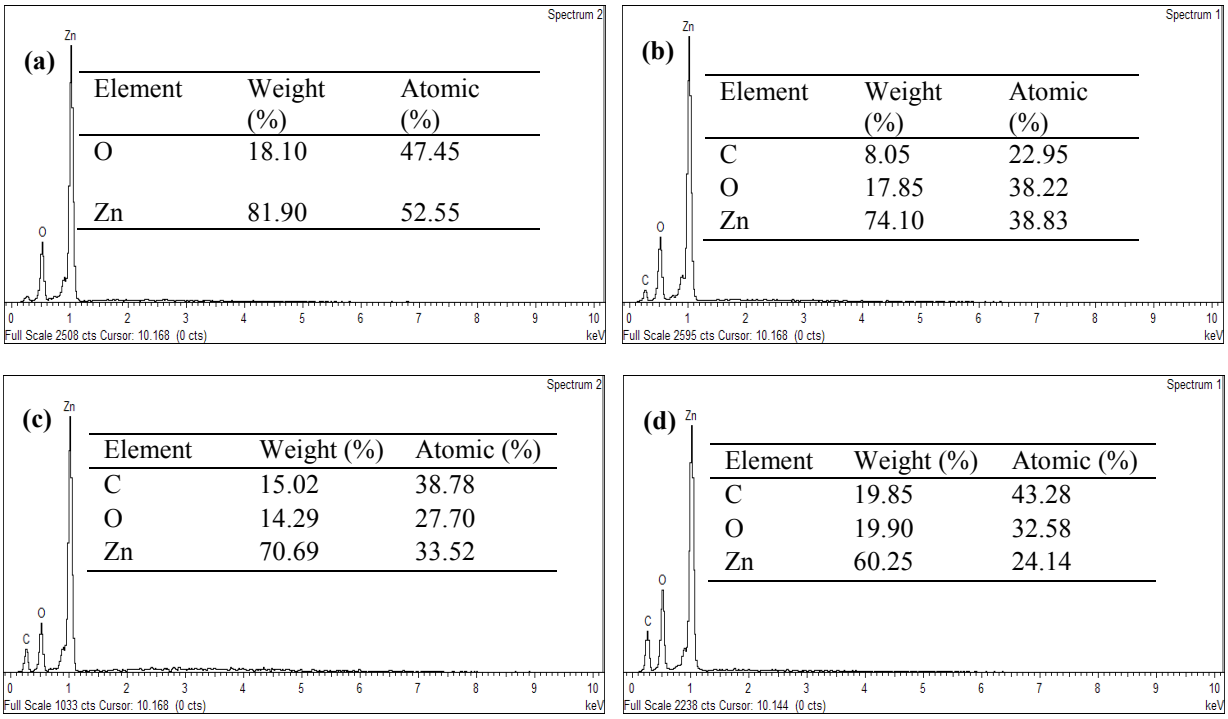

Figure 4. EDX spectra of (a) ZnO, (b) ZnO/rGO5, (c) ZnO/rGO10 and (d) ZnO/rGO20

Surface area and porosity

The BET surface areas of the ZnO and ZnO/rGO nanohybrid photocatalysts were obtained from the nitrogen adsorption- desorption isotherm and the results are represented in Table 1. Both the ZnO and ZnO/rGO nanohybrid photocatalysts met the type V N_2 adsorption- desorption isotherms with H3 hysteresis loop where there was a weak adsorbent- adsorbate interaction. The high adsorption at a relative pressure P/P_0 close to 1.0 also suggested the formation of large mesopores and macropores. Meanwhile, the presence of type H3 loop suggested the occurrence of macropores which are not completely filled with pore condensate [27]. It was observed that there was an improvement in the surface area of the ZnO/rGO nanohybrids compared to ZnO where graphene was incorporated. The nanohybrids were expected to have better photocatalytic performance than ZnO as the high surface area enhanced the efficient adsorption and transfer of organic molecules in a photochemical reaction via π-π conjugation between the organic molecules and graphene sheet [28].

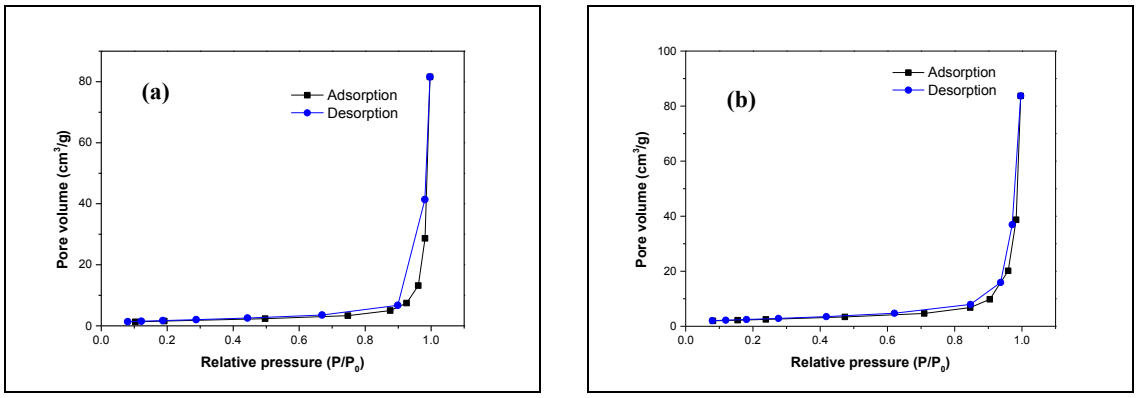

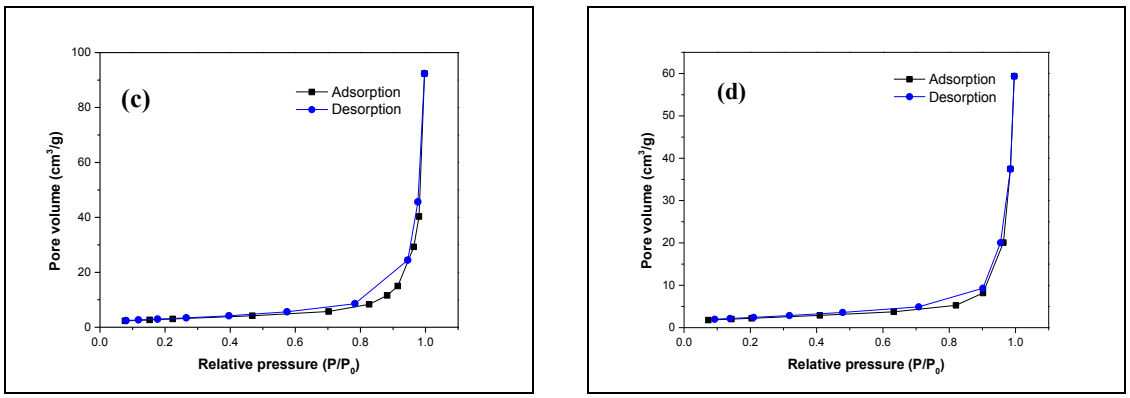

Figure 5. Nitrogen adsorption-desorption isotherm of (a) ZnO (b) ZnO/rGO5 (c) ZnO/rGO10 and (d) ZnO/rGO20

Raman spectroscopy

Figure 6 shows the Raman spectra of GO, rGO and ZnO/rGO10. The characteristic Raman peaks of all three samples showed similar D and G band structures of carbon, which was 1362 cm^{-1} and 1605 cm^{-1}; 1352 cm^{-1} and 1605 cm^{-1}; 1355 cm^{-1} and 1605 cm^{-1} for GO, rGO and ZnO/rGO10, respectively. The D band refers to the presence of disorder in the graphene structure while the G band refers to the presence of an sp^2 carbon type structure [29]. The D band in ZnO/rGO10 was slightly blue shifted by 7 cm^{-1} compared to GO. This was due to the interaction between ZnO and rGO [28]. Similar D and G bands for rGO and ZnO/rGO10 also suggested that the structure of rGO was maintained in the nanohybrid. However, there was a change in the electronic conjugation state of the GO as indicated by the change in the G and D band intensities after being incorporated into ZnO [12, 30]. The intensity ratios (I_D/I_G) increased from 0.87 in GO to 0.98 in ZnO/rGO10 implying that the GO was successfully reduced and more sp^2 domains (graphene sheets) had formed [31]. This also indicated that the introduction of ZnO increased the defects or disorders in the GO sheet [32], hence confirming the formation of the ZnO/rGO nanohybrid.

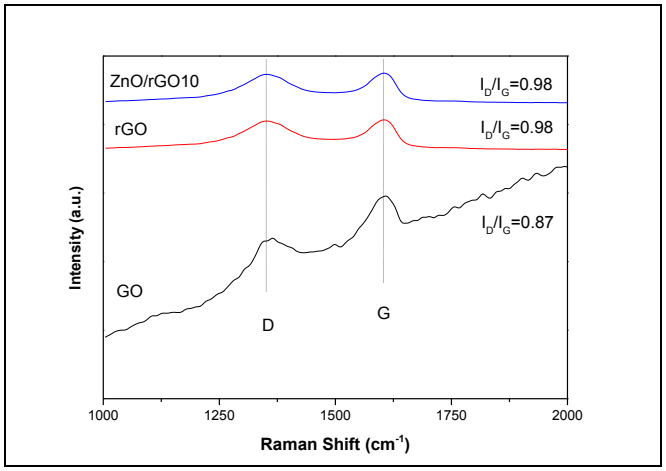

Figure 6. Raman spectra of GO, rGO and ZnO/rGO10

UV- visible diffuse reflectance spectroscopy

Figure 7 shows that both ZnO and ZnO/rGO nanohybrids had similar maximum absorptions at 360 nm. There was an enhancement in the absorption intensity of the ZnO/rGO nanohybrids corresponding to the increase in GO

content in both the UV and visible regions as a result of the increase in the surface electric charge of the oxides and the modification of the fundamental process of electron- hole pair formation during irradiation [33, 34]. The band gap energy of both ZnO and ZnO/rGO nanohybrids were determined by the extrapolation of the linear relationship between $(\alpha hv)^2$ and hv [35]:

$$(\alpha hv)^2 = K\ (hv\ -\ E_g) \tag{1}$$

where α is the absorption coefficient, K is the proportionality constant and v is the frequency of photons.

A plot of $(\alpha hv)^2$ as a function of photon energy, hv for all samples is illustrated in Figure 7 with the band gap values listed in Table 1. The band gap energy of pure ZnO was slightly higher than that of the ZnO/rGO nanohybrids. The reduction in band gap energy could be attributed to the formation of Zn-O-C chemical bonds in the nanohybrid [17, 36, 37]. This also indicated that the presence of graphene influenced the electronic energy level of the ZnO nano-particles. As the band gap energy reduced, more photons were prone to be absorbed by the nanohybrid which in turn would enhance the photocatalytic efficiency.

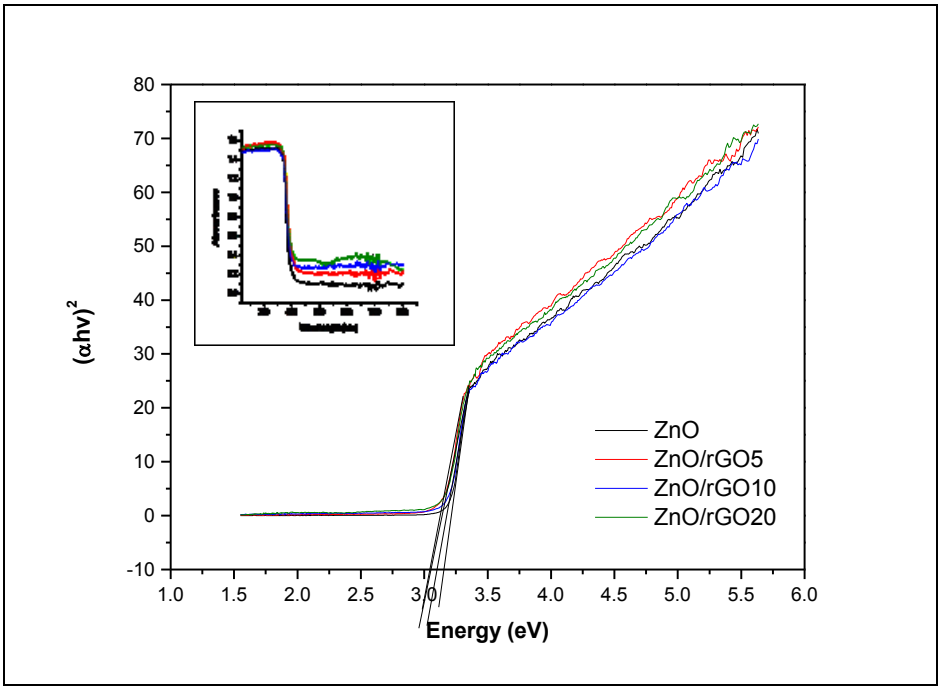

Figure 7. The plots of $(\alpha hv)^2$ versus hv and UV spectrum (inset) for ZnO, ZnO/rGO5, ZnO/rGO10 and ZnO/rGO20

Photocatalytic activities

The photocatalytic performance of both the ZnO and ZnO/rGO nanohybrid photocatalysts were evaluated by degrading methyl orange under the irradiation of UV light and the results are depicted in Figure 8. By comparison, only 53% of MO was degraded using pure ZnO after 180 minutes of irradiation. However, the ZnO/rGO nanohybrids were found to show more prominent photocatalytic efficiency, with 80%, 97% and 77% of MO photodegraded for ZnO/rGO5, ZnO/rGO10, and ZnO/rGO20, respectively.

In principle, the photocatalytic degradation of MO by ZnO and ZnO/rGO nanohybrids is an interface process and follows the Langmuir-Hinshelwood model where it obeys the following assumptions: (i) limited adsorption sites on the catalyst's surface, (ii) monolayer coverage of the catalyst surface with single adsorptions on each site, (iii) reversible adsorption reactions, (iv) homogeneous catalyst surface and (v) zero interactions between the molecules

adsorbed[38]. In this study, H_2O, O_2 and dye (MO) were adsorbed on the surface of the catalyst in adjacent sites. The reaction then occurred between the adsorbed molecules and the radicals generated before the products (CO_2 and H_2O) were desorbed from the catalyst's surface.

$$ZnO + h\nu \rightarrow e_{CB^-} + h^+_{VB} \quad (2)$$

$$H_2O + h^+_{VB} \rightarrow OH\bullet + H^+ \quad (3)$$

$$O_{2(ads)} + eCB^- \rightarrow O_2^{\bullet -} \quad (4)$$

$$OH^-_{(ads)} + h^+_{VB} \rightarrow OH_{(ads)}\bullet \quad (5)$$

$$OH_{(ads)}\bullet + OH\bullet \rightarrow H_2O_2 \quad (6)$$

$$H_2O_2 + O_2^{\bullet -} \rightarrow OH\bullet + OH^- + O_2 \quad (7)$$

$$Dye_{(ads)} + OH\bullet \rightarrow CO_2 + H_2O \quad (8)$$

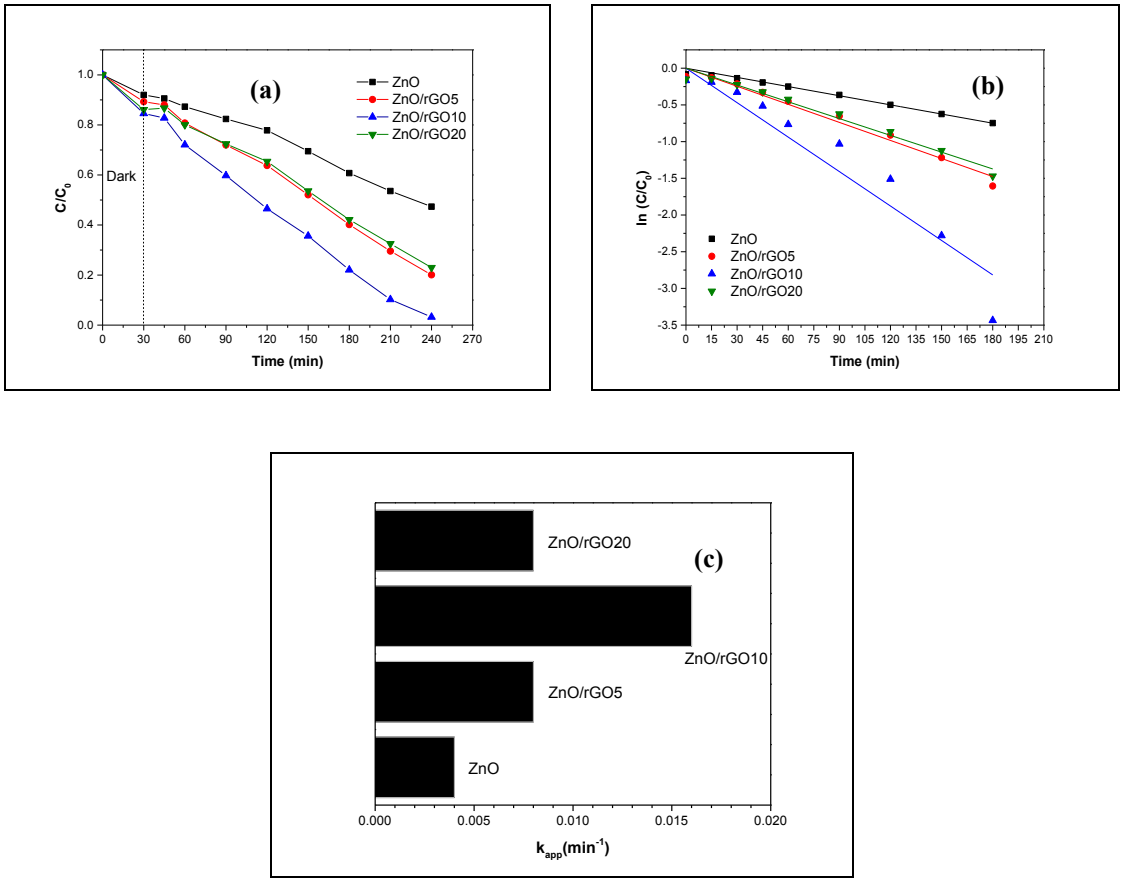

Figure 8. Photodegradation of MO by pure ZnO and ZnO/rGO nanohybrid photocatalysts: (a) reaction profile (b) kinetics and (c) apparent rate constant [condition: 0.5 g of photocatalyst, 10 ppm MO, pH = 6.6]

The data for the photocatalytic degradation of MO was fitted to the Langmuir-Hinshelwood kinetics model and the plot of $\ln(C/C_0)$ vs time (Figure 8b) showed that the photodegradation of MO followed a pseudo first order reaction. The pseudo first order kinetics for MO degradation was calculated as follows:

$$\ln(C/C_0) = \_kt \quad (9)$$

where C (mg/L) is the initial concentration of MO, C_0 (mg/L) is the concentration of MO at time t (min) and *k* (min^{-1}) is the pseudo first order rate constant. The apparent rate constants, k_{app}, were determined from the slope of the plot and is illustrated in Figure 8c. It was clear that the ZnO/rGO nanohybrid photocatalysts exhibited higher photocatalytic activities than pure ZnO. The photocatalytic activity increased as the GO content increased until it reaches the optimum, in the order of ZnO/rGO10 > ZnO/rGO5 > ZnO/rGO20 > ZnO. ZnO/rGO10 had the best photocatalytic activity with a kinetic rate constant 0.016 min^{-1}, which was four times higher than pure ZnO. The results were comparable with that reported in literature [21, 28].

The enhancement in the photocatalytic performance of the ZnO/rGO nanohybrids could be attributed to the strong interactions between ZnO and rGO and the defect sites of graphene. Graphene, with a two- dimensional conjugation structure [39], acted as an excellent electron acceptor. When ZnO was irradiated with UV light, the electrons were excited from the valence band to the conduction band, leaving behind holes in the valence band. These excited electrons could also be transferred from the conduction band of ZnO to the graphene sheet. The effective transfer of photoelectrons from the conduction band of ZnO to graphene prolonged the electron-hole pairs recombination hence promoting the separation of electron- hole pairs of ZnO [40, 41]. More charge carriers were produced from the reactive species which eventually helped in the degradation of MO [42]. The schemetic mechanism of the photocatalysis is shown in Figure 9. Moreover, the ZnO/rGO nanohybrid had a smaller particle size, larger surface area and lower band gap energy compared to ZnO. Such structural changes in ZnO increased the light absorption and the adsorption of MO on the surface of the catalyst; hence increasing the photocatalytic activity of the photocatalysts. However, a high content of GO (ZnO/rGO20) led to a decrement in the photocatalytic activity. Gayathri and co-workers [43] have reported that, at a higher graphene content, the graphene sheets tended to clasp together and appeared like multi-layer graphene after heat treatment. Excess GO also caused a shielding of the active sites on the catalyst surface, and led to the scattering of photons [31, 44, 45]. Since the light absorption of the photocatalyst was reduced, the excitation efficiency of ZnO was also lowered, consequently reducing the photocatalytic activity of the photocatalysts.

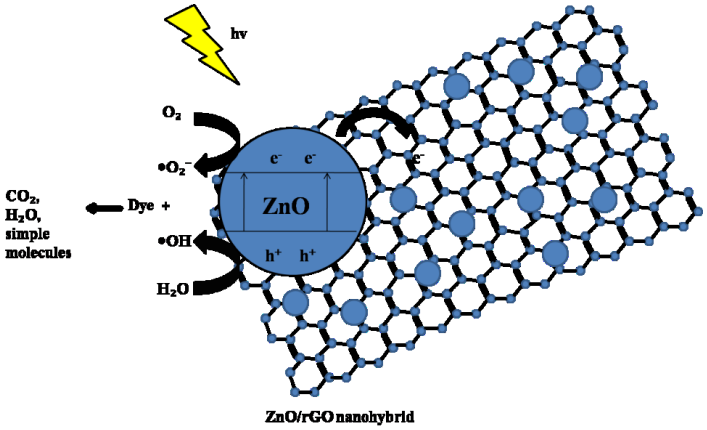

Figure 9. Mechanism of photodegradation

Conclusion

A series of ZnO/rGO nanohybrids with different GO content was successfully synthesized via a simple and inexpensive precipitation method. The ZnO particles were formed on the surface of the graphene sheet. The presence of GO during the synthesis inhibited the crystal growth of ZnO that led to the formation of smaller-sized ZnO particles. ZnO/rGO nanohybrids showed better photodegradation activity compared to ZnO in degrading methyl orange due to their smaller particle sizes and lower band gap energy. ZnO/rGO10 exhibited the highest photocatalytic activity with a kinetic rate constant that was four times higher than pure ZnO. The enhanced photocatalytic activity of the nanohybrids could be attributed to the presence of rGO, an excellent electron acceptor

which enhanced the active transfer of photogenerated electrons of ZnO to the rGO sheet, thereby retarding the charge carrier recombination, thus enhancing the charge separation.

Acknowledgements

The authors would like to thank Universiti Putra Malaysia (UPM) and the Malaysian Government under the Malaysian Exploratory Research Grant Scheme (ERGS-5527187) and UPM-Graduate Research Fellowship award for the financial support for this work.

References

1. Zainal, Z., Hui, L. K., Hussein, M. Z., Taufiq-Yap, Y. H., Abdullah, A. H. and Ramli, I. (2005). Removal of dyes using immobilized titanium dioxide illuminated by fluorescent lamps. *Journal of Hazardous Materials,* 125(1): 113 - 120.
2. Lin, W.-C., Yang, W.-D. and Jheng, S.-Y. (2012). Photocatalytic degradation of dyes in water using porous nanocrystalline titanium dioxide. *Journal of the Taiwan Institute of Chemical Engineers,* 43(2): 269 - 274.
3. Chowdhury, S. and Balasubramanian, R. (2014). Graphene/semiconductor nanocomposites (GSNs) for heterogeneous photocatalytic decolorization of wastewaters contaminated with synthetic dyes: A review. *Applied Catalysis B: Environmental,* 160: 307 - 324.
4. Palanisamy, B., Babu, C., Sundaravel, B., Anandan, S. and Murugesan, V. (2013). Sol–gel synthesis of mesoporous mixed Fe_2O_3/TiO_2 photocatalyst: Application for degradation of 4-chlorophenol. *Journal of Hazardous Materials,* 252: 233 - 242.
5. Ahmad, M., Ahmed, E., Hong, Z., Xu, J., Khalid, N., Elhissi, A. and Ahmed, W. (2013). A facile one-step approach to synthesizing ZnO/graphene composites for enhanced degradation of methylene blue under visible light. *Applied Surface Science,* 274: 273 - 281.
6. Shaari, N., Tan, S. and Mohamed, A. (2012). Synthesis and characterization of CNT/Ce-TiO_2 nanocomposite for phenol degradation. *Journal of Rare Earths,* 30(7): 651 - 658.
7. Zhu, L.-P., Liao, G.-H., Huang, W.-Y., Ma, L.-L., Yang, Y., Yu, Y. and Fu, S.-Y. (2009). Preparation, characterization and photocatalytic properties of ZnO-coated multi-walled carbon nanotubes. *Materials Science and Engineering: B,* 163(3): 194 - 198.
8. Klanwan, J., Akrapattangkul, N., Pavarajarn, V., Seto, T., Otani, Y. and Charinpanitkul, T. (2010). Single-step synthesis of MWCNT/ZnO nanocomposite using co-chemical vapor deposition method. *Materials Letters,* 64(1): 80 - 82.
9. Saleh, T. A., Gondal, M., Drmosh, Q., Yamani, Z. and Al-Yamani, A. (2011). Enhancement in photocatalytic activity for acetaldehyde removal by embedding ZnO nano particles on multiwall carbon nanotubes. *Chemical Engineering Journal,* 166(1): 407 - 412.
10. Sakthivel, S., Geissen, S.-U., Bahnemann, D., Murugesan, V. and Vogelpohl, A. (2002). Enhancement of photocatalytic activity by semiconductor heterojunctions: α-Fe_2O_3, WO_3 and CdS deposited on ZnO. *Journal of Photochemistry and Photobiology A: Chemistry,* 148(1): 283 - 293.
11. Li, B., Liu, T., Wang, Y. and Wang, Z. (2012). ZnO/graphene-oxide nanocomposite with remarkably enhanced visible-light-driven photocatalytic performance. *Journal of Colloid and Interface Science,* 377(1): 114 - 121.
12. Wang, Z.-I., Xu, D., Huang, Y., Wu, Z., Wang, L.-M. and Zhang, X.-B. (2012). Facile, mild and fast thermal-decomposition reduction of graphene oxide in air and its application in high-performance lithium batteries. *Chemical Communications,* 48(7): 976 - 978.
13. Liu, Y., Han, G., Li, Y. and Jin, M. (2011). Flower-like zinc oxide deposited on the film of graphene oxide and its photoluminescence. *Materials Letters,* 65(12): 1885 - 1888.
14. Ameen, S., Akhtar, M. S., Seo, H.-K. and Shin, H. S. (2013). Advanced ZnO–graphene oxide nanohybrid and its photocatalytic applications. *Materials Letters,* 100: 261 - 265.
15. Zhou, X., Shi, T. and Zhou, H. (2012). Hydrothermal preparation of ZnO-reduced graphene oxide hybrid with high performance in photocatalytic degradation. *Applied Surface Science,* 258(17): 6204 -6211.
16. Leng, Y., Wang, W., Zhang, L., Zabihi, F. and Zhao, Y. (2014). Fabrication and photocatalytical enhancement of ZnO-graphene hybrid using a continuous solvothermal technique. *The Journal of Supercritical Fluids,* 91: 61 - 67.

17. Xu, S., Fu, L., Pham, T. S. H., Yu, A., Han, F. and Chen, L. (2015). Preparation of ZnO flower/reduced graphene oxide composite with enhanced photocatalytic performance under sunlight. *Ceramics International,* 41(3): 4007 - 4013.
18. Marlinda, A., Huang, N. M., Muhamad, M. R., An'amt, M., Chang, B. Y. S., Yusoff, N., Harrison, I., Lim, H. N., Chia, C. and Kumar, S.V. (2012). Highly efficient preparation of ZnO nanorods decorated reduced graphene oxide nanocomposites. *Materials Letters,* 80: 9 - 12.
19. Fu, D., Han, G., Chang, Y. and Dong, J. (2012). The synthesis and properties of ZnO–graphene nano hybrid for photodegradation of organic pollutant in water. *Materials Chemistry and Physics,* 132(2): 673 - 681.
20. Ming, H. N. (2010). Simple room-temperature preparation of high-yield large-area graphene oxide. *International Journal of Nanomedicine,* 6: 3443 - 3448.
21. Zhang, Y., Chen, Z., Liu, S. and Xu, Y.-J. (2013). Size effect induced activity enhancement and anti-photocorrosion of reduced graphene oxide/ZnO composites for degradation of organic dyes and reduction of Cr(VI) in water. *Applied Catalysis B: Environmental,* 140: 598 - 607.
22. Chen, Y.-L., Hu, Z.-A., Chang, Y.-Q., Wang, H.-W., Zhang, Z.-Y., Yang, Y.-Y. and Wu, H.-Y. (2011). Zinc oxide/reduced graphene oxide composites and electrochemical capacitance enhanced by homogeneous incorporation of reduced graphene oxide sheets in zinc oxide matrix. *The Journal of Physical Chemistry C,* 115(5): 2563 - 2571.
23. Moussa, H., Girot, E., Mozet, K., Alem, H., Medjahdi, G. and Schneider, R. (2016). ZnO rods/reduced graphene oxide composites prepared via a solvothermal reaction for efficient sunlight-driven photocatalysis. *Applied Catalysis B: Environmental,* 185: 11 - 21.
24. Samadi, M., Shivaee, H. A., Zanetti, M., Pourjavadi, A. and Moshfegh, A. (2012). Visible light photocatalytic activity of novel MWCNT-doped ZnO electrospun nanofibers. *Journal of Molecular Catalysis A: Chemical,* 359: 42 - 48.
25. Kuo, S.-Y., Chen, W.-C., Lai, F.-I., Cheng, C.-P., Kuo, H.-C., Wang, S.-C. and Hsieh, W.-F. (2006). Effects of doping concentration and annealing temperature on properties of highly-oriented Al-doped ZnO films. *Journal of Crystal Growth,* 287(1): 78 - 84.
26. Selvam, N. C. S., Narayanan, S., Kennedy, L. J. and Vijaya, J. J. (2013). Pure and Mg-doped self-assembled ZnO nano-particles for the enhanced photocatalytic degradation of 4-chlorophenol. *Journal of Environmental Sciences,* 25(10): 2157 - 2167.
27. Thommes, M., Kaneko, K., Neimark, A. V., Olivier, J. P., Rodriguez-Reinoso, F., Rouquerol, J. and Sing, K. S. (2015). Physisorption of gases, with special reference to the evaluation of surface area and pore size distribution (IUPAC Technical Report). *Pure and Applied Chemistry,* 87 (9-10): 1051 - 1069.
28. Kavitha, M., Pillai, S. C., Gopinath, P. and John, H. (2015). Hydrothermal synthesis of ZnO decorated reduced graphene oxide: Understanding the mechanism of photocatalysis. *Journal of Environmental Chemical Engineering*, 3:1194 - 1199.
29. Omar, F. S., Nay Ming, H., Hafiz, S. M. and Ngee, L. H. (2014). Microwave synthesis of zinc oxide/reduced graphene oxide hybrid for adsorption-photocatalysis application. *International Journal of Photoenergy,* 2014: 1 - 8.
30. Huang, K., Li, Y., Lin, S., Liang, C., Wang, H., Ye, C., Wang, Y., Zhang, R., Fan, D. and Yang, H. (2014). A facile route to reduced graphene oxide–zinc oxide nanorod composites with enhanced photocatalytic activity. *Powder Technology,* 257: 113 - 119.
31. Peng, Y., Ji, J. and Chen, D. (2015). Ultrasound assisted synthesis of ZnO/reduced graphene oxide composites with enhanced photocatalytic activity and anti-photocorrosion. *Applied Surface Science,* 356: 762 - 768.
32. Song, Y., Shao, P., Tian, J., Shi, W., Gao, S., Qi, J., Yan, X. and Cui, F. (2016). One-step hydrothermal synthesis of ZnO hollow nanospheres uniformly grown on graphene for enhanced photocatalytic performance. *Ceramics International,* 42(1): 2074 - 2078.
33. Lv, T., Pan, L., Liu, X., Lu, T., Zhu, G. and Sun, Z. (2011). Enhanced photocatalytic degradation of methylene blue by ZnO-reduced graphene oxide composite synthesized via microwave-assisted reaction. *Journal of Alloys and Compounds,* 509(41): 10086 - 10091.
34. Nipane, S., Korake, P. and Gokavi, G. (2015). Graphene-zinc oxide nanorod nanocomposite as photocatalyst for enhanced degradation of dyes under UV light irradiation. *Ceramics International,* 41 (3): 4549 - 4557.
35. Yakuphanoglu, F. (2010). Electrical characterization and device characterization of ZnO microring shaped films by sol–gel method. *Journal of Alloys and Compounds,* 507(1): 184 - 189.

36. Tien, H. N., Khoa, N. T., Hahn, S. H., Chung, J. S., Shin, E. W. and Hur, S. H. (2013). One-pot synthesis of a reduced graphene oxide–zinc oxide sphere composite and its use as a visible light photocatalyst. *Chemical Engineering Journal,* 229: 126 - 133.
37. Morales-Torres, S., Pastrana-Martínez, L. M., Figueiredo, J. L., Faria, J. L. and Silva, A. M. (2013). Graphene oxide-P25 photocatalysts for degradation of diphenhydramine pharmaceutical and methyl orange dye. *Applied Surface Science,* 275: 361 - 368.
38. Khezrianjoo, S. and Revanasiddappa, H. (2012). Langmuir-Hinshelwood kinetic expression for the photocatalytic degradation of Metanil Yellow aqueous solutions by ZnO catalyst. *Chemical Sciences Journal,* 3: 1 - 7.
39. Liu, Q., Liu, Z., Zhang, X., Yang, L., Zhang, N., Pan, G., Yin, S., Chen, Y. and Wei, J. (2009). Polymer photovoltaic cells based on solution-processable graphene and P3HT. *Advanced Functional Materials,* 19(6): 894 - 904.
40. Yang, Y. and Liu, T. (2011). Fabrication and characterization of graphene oxide/zinc oxide nanorods hybrid. *Applied Surface Science,* 257(21): 8950 - 8954.
41. Herring, N. P., Almahoudi, S. H., Olson, C. R. and El-Shall, M. S. (2012). Enhanced photocatalytic activity of ZnO–graphene nanocomposites prepared by microwave synthesis. *Journal of Nanoparticle Research,* 14(12): 1 - 13.
42. Wang, X., Zhi, L. and Müllen, K. (2008). Transparent, conductive graphene electrodes for dye-sensitized solar cells. *Nano Letters,* 8(1): 323 - 327.
43. Gayathri, S., Jayabal, P., Kottaisamy, M. and Ramakrishnan, V. (2014). Synthesis of ZnO decorated graphene nanocomposite for enhanced photocatalytic properties. *Journal of Applied Physics,* 115(17): 173504.
44. Chen, Z., Zhang, N., and Xu, Y.-J. (2013). Synthesis of graphene–ZnO nanorod nanocomposites with improved photoactivity and anti-photocorrosion. *CrystEngComm,* 15(15): 3022 - 3030.
45. Sarkar, S. and Basak, D. (2013). The reduction of graphene oxide by zinc powder to produce a zinc oxide-reduced graphene oxide hybrid and its superior photocatalytic activity. *Chemical Physics Letters,* 561: 125 - 130.